

# Analysis of Channel Access Priority Classes in LTE-LAA Spectrum Sharing System\*

Yao Ma

Communications Technology Laboratory,  
National Institute of Standards and Technology  
325 Broadway, Boulder, Colorado, USA

**Abstract**— To provide differentiated quality of service in long-term evolution (LTE) license assisted access (LAA) procedure, the 3GPP has defined several channel access priority classes (CAPCs). They use distinct arbitration inter-frame space (AIFS), contention window (CW) size, and payload duration. While evaluating the effects of CW size and payload duration is relatively straightforward, accurately modelling and analyzing the effect of AIFS has not been satisfactorily addressed. Available methods on analyzing different AIFSs are accurate for only limited parameter setups, or involve systematic approximations. Different from existing results, we develop a *non-homogeneous* per-slot Markov chain model to represent the state of each priority class during and after the AIFS, and analyze the channel access probability (CAP), successful transmission probability (STP), and average throughput of each class. Some novel features of our method include: 1) we model and solve the per-slot class-dependent link statistics (such as CAP and STP), which vary based on the slot location; and 2) we provide an in-depth analysis on the average throughput, and design a multi-class combinatorial procedure to evaluate average time spent per successful transmission on each delay cell. We program the LAA CAPC algorithms and implement extensive Monte Carlo simulations, which validate the accuracy of our analytical results even in very low throughput region for lower priority classes, and demonstrate the effects of AIFS and other parameters in an LAA system. These results provide solid progress for evaluating priority classes in the LTE-LAA system and other spectrum sharing systems, and can be extended to support system and parameter optimization.

Keywords: Channel Access Priority Classes, CSMA/CA, LTE-LAA, QoS Differentiation, Spectrum Sharing, Throughput

## I. INTRODUCTION

To enable constructive coexistence between the long-term evolution (LTE) and incumbent systems, such as IEEE 802.11 wireless local area network (WLAN) in the unlicensed industrial, scientific, and medical (ISM) radio band, the 3rd Generation Partnership Project (3GPP) has specified a license assisted access (LAA) procedure [1]–[4]. To provide differentiated quality of service (QoS) for diverse applications (such as audio, video and background services), the recent 3GPP LAA specification [3] includes several channel access priority classes (CAPCs). These classes use carrier sense multiple access with collision avoidance (CSMA/CA), and have different channel access parameters, such as arbitrary inter-frame space (AIFS), contention window (CW) size, and transmit opportunity (TXOP) payload duration.

The AIFS for a CAPC is defined as the required silent duration after a channel busy event is over and before the backoff process is resumed. The AIFS is composed of a short IFS (SIFS) duration and several additional idle slots which are distinct for each CAPC [3]. The LTE-LAA specification [3] did not provide a name for this parameter, and we term it “AIFS” due to its conceptual equivalence (or high similarity) to a popular term used in the enhanced distributed channel access (EDCA) procedure of the IEEE 802.11 WLAN standard [5], [6]. A CAPC with higher priority uses a shorter AIFS, and the effect of adjusting AIFS is typically more significant than that achieved by adjusting the CW size. Besides 3GPP LAA channel access [3] and IEEE WLAN EDCA specifications [5], the European Telecommunications Standards Institute (ETSI) has recently introduced distinct AIFSs in different priority classes to provide differentiated QoS in its unlicensed spectrum access procedure [7].

Evaluating the effects of CW size and payload duration is relatively straightforward based on abundant available methods in LAA-based spectrum sharing systems [8]–[13]. In these works, the AIFS is not considered, or equivalently, assumed to be identical for all types of transmissions. In [14]–[17], several optimization schemes for LAA and WLAN coexistence systems are developed. Especially, [14], [16], [17] have considered use of a shorter idle channel wait timing than the WLAN counterpart to dominate the channel access, and provide fairness and/or throughput optimization.

To date, accurately modelling and analyzing the performance of CAPCs with different AIFSs is still a challenging task, and has yet to be rigorously addressed. In this paper, following the recent 3GPP LAA specification on the CAPCs [3], we provide a new performance analysis that is valid for a wide range of practical CSMA/CA parameters, including distinct AIFS numbers. The contributions and novelty of this paper are highlighted as follows:

- We develop a *non-homogeneous* Markov chain to model and compute the system channel access probability (SCAP) and other statistics at each delay cell after the channel busy event and SIFS.
- We analyze the CAP, STP, and average throughput of each CAPC link as functions of AIFS, and other CSMA/CA parameters. The result is accurate or a good approximation for the parameter ranges studied, including the important cases such as small CW sizes and non-trivial

\*U.S. Government work, not subject to U.S. copyright.

differences in AIFS numbers, as considered by an LAA specification [3].

- We implement algorithm programming and extensive simulation to evaluate the coexistence performance of multiple CAPCs. Numerical results validate the accuracy of our analytical results, and demonstrate the effects of AIFS, CW, and payload of each priority class in an LAA downlink system.

This result is significant because it allows us to accurately evaluate the differentiated QoS and channel access performance of LAA priority classes for critical parameter ranges, and the evaluation involves only a low to moderate complexity. Our method can be easily extended to provide performance analysis and support parameter optimization in other spectrum sharing systems and specifications. Examples include priority classes for unlicensed spectrum access defined by ETSI, and coexisting LTE-LAA and IEEE 802.11 WLAN systems.

## II. RELATED WORK

Analytical results addressing distinct AIFSs in the LAA or ETSI unlicensed access systems are rare to find, if available at all. Next, we briefly review a few state-of-the-art results in the analysis of the WLAN EDCA procedure [18]–[22]. The work discussed in [18]–[20] develop different AIFS zone models for performance analysis. Several major or minor approximations are involved in computing the channel access and successful transmission probabilities. In [18] a renewal process between transmissions is modelled, and the analysis assumes that the channel access probability (CAP) of each class is constant along the slots, which involves an approximation. A highly complicated multi-dimensional Markov chain model is developed in [19], and a simplified model is provided in [20] for the QoS control. In [19] the authors model the channel idle probability for each class to be constant within each AIFS zone. In [20] they assume that the throughput of each CAPC link is inversely proportional to its backoff wait time, and model the CAP for each link to be a constant along slot index. In [21] the authors seek to provide an analytical result that does not consider the per-slot differences after the SIFS. Instead, they use a model with a constant transmission probability per class. This result may be regarded as a good approximation under conditions that the CW sizes of all classes are large and differences between AIFSs are small.

In [22], based on an extension of the results in [23], the authors model the effect of different AIFSs by a power term of a successful transmission probability (STP), aka.  $P_T^{\Delta_{\text{AIFS}}}$ , where  $P_T$  is the STP averaged over all links and all idle slots, and  $\Delta_{\text{AIFS}}$  is the AIFS difference between classes of the highest priority and the considered class. This modelling method is simple and elegant, but it involves approximations: the STPs of different classes are approximated as a single STP term; furthermore, this STP is modelled as a constant along the  $\Delta_{\text{AIFS}}$  slot duration. Thus, it only partially captures the effect of distinct AIFS, and involves approximations which can be observed from simulation results in [22], especially for low-priority classes.

TABLE I: Definitions of some symbols frequently used in this paper.

Symbol	Definition
CAP	Channel access probability (per link)
CAPC	Channel access priority class
SCAP	System channel access probability
STP	Successful transmission probability
$\tau_{c,d_c}$	CAP of class $c$ at delay index $d_c$
$P_{\text{ex},S}$	SCAP at delay cell index $S$
$P_{c,d_c,T}$	Conditional STP of class $c$ at delay index $d_c$
$P_{\text{suc},c,S}$	Unconditional STP of class $c$ at cell index $S$

In summary, the above-mentioned results provide various analytical techniques for evaluating the impact of distinct AIFS on the achieved differential QoS performance in WLAN EDCA systems. A common weakness of these methods is that the per-slot difference due to distinct AIFS is not adequately modelled. Consequently, the reliability of applying these methods for assessing performance of lower priority classes at small throughput region is unclear or questionable. Systematic approximations may rise by extending available methods to model and evaluate the different CAPCs. It remains a challenging technical problem to accurately model and evaluate effects of different parameter setups and achievable performance of distinct priority classes in the LTE-LAA, ETSI and other spectrum sharing scenarios.

For ease of reference, some symbols that are frequently used in this paper are listed in Table I.

## III. SYSTEM MODEL

We assume that in a downlink LAA system, there are  $C_{\text{max}}$  active CAPC groups, with  $n_c$  links for group  $c$ , with  $c = 1, 2, 3, C_{\text{max}}$  and  $C_{\text{max}} = 4$ . Each link has a fully backlogged traffic. To provide differentiated QoS for different types of services, a recent 3GPP release [3] has defined four LAA channel access priority classes, as shown in Table II. Throughout this paper, we use terms ‘‘CAPC’’ and ‘‘class’’ interchangeably. Each class has a different defer period after a channel busy event (we term it AIFS in this paper), besides distinct CW size and TXOP duration. The AIFS duration of each link in class  $c$  is given by

$$T_{c,\text{AIFS}} = T_{\text{SIFS}} + A_c T_{sl}, \quad (1)$$

where  $T_{\text{SIFS}} = 16\mu\text{s}$ , and  $T_{sl}$  is a backoff idle slot duration with  $T_{sl} = 9\mu\text{s}$ , and  $A_c$  is called the AIFS number of class  $c$ . Based on Table II,  $A_c \in \{1, 1, 3, 7\}$  for classes 1-4. Let CAPC  $c$  have 0 to  $K_c$  backoff stages. From Table II, it is obvious that  $K_1 = K_2 = 1$ ,  $K_3 = 2$ ,  $K_4 = 6$ . Let  $W_{c,k}$  be the CW size of class  $c$  at stage  $k$ . Since the CW value listed in Table II is equal to  $W_{c,k} - 1$ , we have  $W_{1,0} = 4, W_{1,1} = 8$  for class 1,  $W_{2,0} = 8, W_{2,1} = 16$  for class 2, and  $W_{3,0} = W_{4,0} = 16$ , etc.

The channel access of all links follows a CSMA/CA procedure defined in Section 15.1.1 of [3]. We briefly summarize

TABLE II: List of channel access parameters of LTE-LAA downlink, adopted from Table 15.1.1-1 of [3].

Class $c$	AIFS number ( $A_c$ )	$CW_{\min}$	$CW_{\max}$	Occupancy Duration
1	1	3	7	2 ms
2	1	7	15	3 ms
3	3	15	63	8 or 10 ms
4	7	15	1023	8 or 10 ms

the procedure below, but make some modifications to improve its clarity (without changing the procedure itself).

#### LAA Channel Access Procedure

Assume a random backoff counter value  $W$  for a class  $c$  link.

- 1) Initialize. If this link finishes a transmission successfully (or just joins the network), set backoff stage  $k = 0$ , and draw a counter value  $W$  uniformly from  $(0, W_{c,0} - 1)$ . Otherwise, if this link finishes a transmission that failed, increase the current stage  $k_{\text{old}}$  by one to obtain  $k_{\text{new}} = \min(k_{\text{old}} + 1, K_c)$ . If  $k_{\text{old}} = K_c$ , then  $k_{\text{new}} = K_c$ . Draw a counter value  $W$  uniformly from  $(0, W_{c,k_{\text{new}}} - 1)$ .
- 2) If  $W = 0$ , starts a transmission. Otherwise, go to 3).
- 3) If  $W > 0$ , do either of the following 2 steps based on the given conditions:
  - 3.1) If a channel busy event was just over, sense the channel for a duration  $T_{c,\text{AIFS}}$ ; If the result is idle, reduce counter  $W$  by one, and go to 2); otherwise, frozen counter due to channel busy, and continue with Step 3.1.
  - 3.2) If the channel continues to be idle for a  $T_{sl}$  duration after a previous counter reduction, reduce counter  $W$  by one, and go to step 2). Otherwise, frozen counter due to channel busy, and go to Step 3.1.

Based on Table II and the LAA channel access procedure, we depict the signal timing after a channel busy event (successful or failed transmission) in Fig. 1. Right after the SIFS, each slot  $T_{sl}$  is called a delay cell, indexed from 0 to  $S_{\max}$ . With Table II, the  $S_{\max}$  is determined by the maximum CW size of class 1, so that  $S_{\max} = 7$  when a class 1 link is active and fully backlogged. When none of the class 1 links are active, but some class 2 links are active, we have  $S_{\max} = 15$ .

#### IV. PERFORMANCE ANALYSIS

Technical flow of this section is described as follows: In the first step, we derive SCAP at each delay cell based on a novel non-homogeneous Markov chain model during and after the AIFS. The SCAP is equivalent to the reset and exit probability at each delay cell. In the second and third steps, we derive the CAP and the STP of a link of each class. The unknowns and equations in these steps are solved jointly to obtain the CAPs and STPs which are distinct among classes and along the delay cells. In the fourth and final step, we derive the average time spent per successful transmission at each delay cell. This involves a complicated multi-class combinatorial evaluation procedure. Then we obtain the average throughput of each class. Each step is built upon results from the previous steps.

#### A. Non-Homogeneous Markov Model for Distinct AIFS

Based on Table II and Fig. 1, we provide a non-homogeneous Markov chain-based model of the LTE-LAA process, depicted in Fig. 2. In Figs. 1 and 2 we use the term “delay cell” for the idle slots after the SIFS instead of “counter” to distinguish it from the backoff counter. We use “delay cell” to model the global timing of all links during the AIFS period, but will use term “backoff counter” to model the individual Markov chain of each link in its channel access procedure.

We show Fig. 2 in order to support the evaluation of the statistics of each class in the spectrum sharing scenario. It is important to analyze the stationary probability of each delay cell  $S_0, \dots, S_{\max}$ , as denoted by  $P_{S_0}, \dots, P_{S_{\max}}$ . Based on Fig. 2, we also define  $P_{S,S+1}$  as the feedforward transition probability from cells  $S$  to  $S + 1$ , and  $P_{\text{ex},S}$  as the SCAP (or exit probability) from cell  $S$  back to cell 0, respectively, for  $S = 1, \dots, S_{\max}$ . Using a precise analysis, we have  $P_{S-1,S} \neq P_{S,S+1}$ , for any  $S$ . Furthermore, as  $S$  increases, the effective CW sizes tend to decrease, causing increased transmission probability. This effect has not been explicitly modelled in available work on analyzing AIFS [18]–[22], but will be addressed in Subsection IV-B. Thus, the probability transition graph in Fig. 2 can be regarded as a new non-homogeneous Markov Model.

Define  $\hat{A}_c$  as the difference between the AIFS numbers of class  $c$  and class 1, which is  $\hat{A}_c = A_c - A_1 = A_c - 1$ . We have  $\hat{A}_1 = \hat{A}_2 = 0$ ,  $\hat{A}_3 = 2$ , and  $\hat{A}_4 = 6$ . We define  $d_c$  as the corresponding delay index (in units of idle slot  $T_{sl}$ ) of the class  $c$  with respect to that of class 1, given by

$$d_c = S - \hat{A}_c, \quad (2)$$

for  $c = 1, 2, 3, 4$ . For example, at cell index  $S = 6$ ,  $d_1 = d_2 = 6$ ,  $d_3 = 4$ , and  $d_4 = 0$ .

Define  $\tau_c(S)$  as the CAP of class  $c$  at cell  $S$ , then

$$\tau_c(S) = \begin{cases} 0 & S < \hat{A}_c \\ \tau_{c,d_c} & S \geq \hat{A}_c, \end{cases} \quad (3)$$

where  $\tau_{c,d_c}$  is the CAP of class  $c$  with delay index  $d_c$ . Define  $P_{I,c}(d_c)$  as the class  $c$  idle probability at its own delay index  $d_c$ . It follows that

$$P_{I,c}(d_c) = (1 - \tau_{c,d_c})^{n_c}. \quad (4)$$

From Fig. 2, we obtain (for  $S = 0, 1, \dots, S_{\max} - 1$ )

$$P_{S,S+1} = P_{I,1}(S - \hat{A}_1)P_{I,2}(S - \hat{A}_2) \cdot P_{I,3}(S - \hat{A}_3)P_{I,4}(S - \hat{A}_4), \quad (5)$$

$$P_S = P_{S_0} \prod_{s=0}^{S-1} P_{s,s+1}. \quad (6)$$

Furthermore, since  $\sum_{d=0}^{S_{\max}} P_{S_d} = 1$ , we obtain the stationary probability of cell 0 as

$$P_{S_0} = \left[ 1 + \sum_{n=1}^{S_{\max}} P_{0,1}P_{1,2} \cdots P_{n-1,n} \right]^{-1}.$$

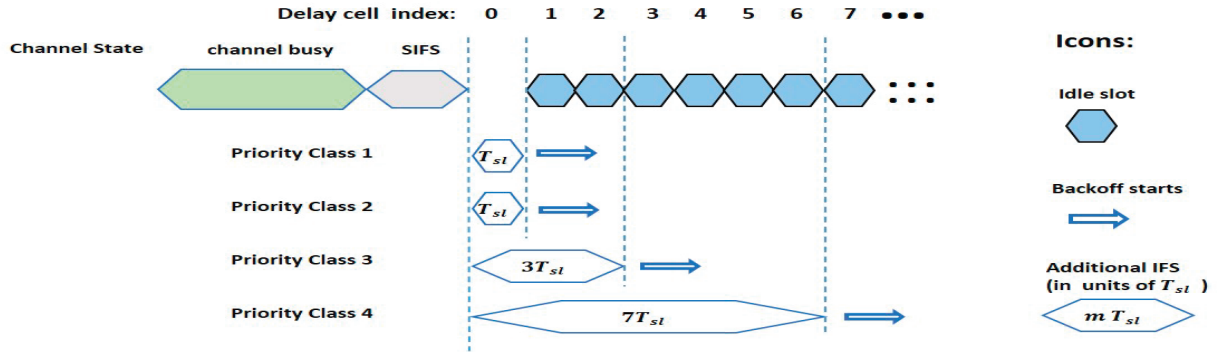


Fig. 1: Our proposed diagram of AIFS in 3GPP downlink LAA procedure for four channel access priority classes. The delay cell index refers to each idle slot after the SIFS but before a new transmission starts.

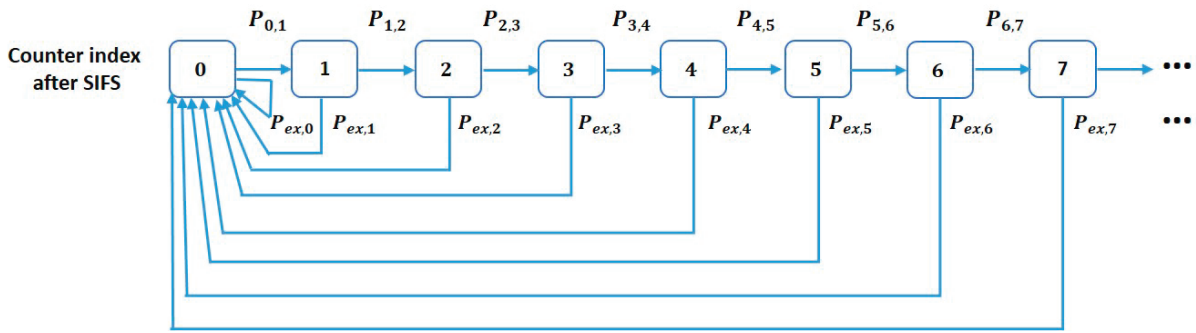


Fig. 2: Illustration of delay cells and the probability transition paths after the SIFS.

Probabilities of other delay cells  $P_S$ ,  $S = 1, \dots, S_{\max}$  follow directly. To solve (5), we need to find the idle probability  $P_{I,c}(d_c)$  for all  $c$  and  $d_c$ , which is studied next.

The system idle probability at cell  $S$  is obtained as

$$P_{I,S} = \prod_{c=1}^C (1 - \tau_c(S))^{n_c}, \quad (7)$$

where  $\tau_c(S)$  is the CAP of class  $c$  at cell  $S$ . Note that  $\tau_c(S)$  can be zero based on the AIFS zones. The SCAP at cell  $S$  is derived as

$$P_{ex,S} = (1 - P_{I,S}) \prod_{s=0}^{S-1} P_{I,s}. \quad (8)$$

### B. Channel Access Probability and STP

In the literature, the CAP is typically modelled as constant in each AIFS zone, and changes only at zone boundary. Here, to be more accurate, we model CAP as variable along delay cell index  $S$ . As  $S$  increases and  $d_c \geq 0$ , before a new transmission starts (aka, reset of cell to 0), the CAP shall increase with  $d_c$ . As  $d_c$  increases, the backoff counter value of every class  $c$  link decreases. To account for this effect, we model the effective CW size at each backoff stage of class  $c$

as

$$\hat{W}_{c,k} = W_{c,k} - d_c. \quad (9)$$

For class  $c$ , the total probability of all the backoff counter states is unity. Therefore,

$$\sum_{k=0}^{K_c} \sum_{l=0}^{\hat{W}_{c,k}} b_{c,k,l} = 1, \quad (10)$$

where  $b_{c,k,l}$  is the probability of backoff counter  $l$  at stage  $k$  for class  $c$ . Note that backoff counter index  $l$  is different from the delay cell index  $S$  after the SIFS, shown in Fig. 2. Using steps similar to those given in [24], we derive the CAP as

$$\tau_{c,d_c} = b_{c,0,0} / P_{c,d_c,T}, \quad (11)$$

where  $P_{c,d_c,T}$  is the conditional STP of class  $c$  at cell  $d_c$ , and

$$b_{c,0,0} = \left[ \sum_{k=0}^{K_c-1} (1 - P_{c,d_c,T})^k (\hat{W}_{c,k} + 1) / 2 + (\hat{W}_{c,K_c} + 1) (1 - P_{c,d_c,T})^{K_c} / (2P_{c,d_c,T}) \right]^{-1}. \quad (12)$$

A major difference between (11) and the CAP given in [24] is that (11) is valid even when the CW size is not a power-of-two integer. Furthermore, our result models the effect of shrinking

CW size as the delay cell index increases. This method is consistent because when  $d_c = W_{c,K_c}$  (for  $c = 1$ ), we have  $\hat{\tau}_{c,d_c} = 1$ , which means that after the maximum possible counter reduction, the CAP must reach unity, as expected. To our knowledge, the majority of available methods have not explicitly modelled this effect.

After  $\tau_{c,d_c}$  (for all  $c$  and  $d_c$ ) is derived, by using Fig. 2, we obtain the STP for a class  $C$  link as

$$\begin{aligned} P_{C,d_c,T} &= (1 - \tau_{C,d_c})^{n_c-1} \prod_{c=1}^{C-1} (1 - \tau_{c,d_c})^{n_c} \\ &= \frac{\prod_{c=1}^4 (1 - \tau_{c,d_c})^{n_c}}{(1 - \tau_{C,d_c})}. \end{aligned} \quad (13)$$

There are  $4(S_{\max} + 1)$  equalities based on (13) for all  $c$  and  $d_c$ . We have the following parameters to be solved:

- CAPs  $\{\tau_{c,d_c}\}$  (which are  $4(S_{\max} + 1)$  unknowns),
- STPs  $\{P_{c,d_c,T}\}$  (which are  $4(S_{\max} + 1)$  unknowns).

Since (11) and (13) provide  $8(S_{\max} + 1)$  equations and involve  $8(S_{\max} + 1)$  unknowns, we can use an iterative search to uniquely solve for the unknowns.

### C. Throughput

Note that SCAP  $P_{ex,S}$  defined in (8) forms a probability set of mutually exclusive events, for  $S = 0, 1, \dots, S_{\max}$ , and  $\sum_{S=0}^{S_{\max}} P_{ex,S} = 1$ . By use of the SCAP set, the average sum throughput of class  $c$  links is given by

$$R_c = \frac{n_c \sum_{S=0}^{S_{\max}} P_{ex,S} P_{suc,c,S} T_{p,c}}{\sum_{S=0}^{S_{\max}} P_{ex,S} T_{ave,S}}, \quad (14)$$

where  $P_{suc,c,S}$  is the unconditional successful transmission probability of a class  $c$  link at cell  $S$ ,  $T_{p,c}$  is payload duration of class  $c$ , and  $T_{ave,S}$  is average time spent to enable a successful transmission at cell  $S$ . It follows that  $P_{suc,c,S} = \tau_{c,d_c} P_{I,S}$ . Since  $\sum_{S=0}^{S_{\max}} P_S = 1$  holds, we provide another formula for class  $c$  sum throughput as:

$$R_c = \frac{n_c \sum_{S=0}^{S_{\max}} P_S P_{suc,c,S} T_{p,c}}{\sum_{S=0}^{S_{\max}} P_S T_{ave,S}}. \quad (15)$$

The  $T_{ave,S}$  is difficult to derive, since it involves interactions among  $C = 4$  classes of links. We obtain

$$T_{ave,S} = \begin{cases} T_{TX,12}(S) & S \in (\hat{A}_2, \hat{A}_3 - 1) \\ T_{TX,123}(S) & S \in (\hat{A}_3, \hat{A}_4 - 1) \\ T_{TX,1234}(S) & S \in (\hat{A}_4, S_{\max}), \end{cases} \quad (16)$$

where  $T_{TX,12}(S)$  is the average channel busy duration to enable one successful transmission when classes 1 and 2 links can resume backoff (and hence possibly transmit) at cell  $S$ . Similarly,  $T_{TX,123}(S)$  and  $T_{TX,1234}(S)$  are the average channel busy durations caused by links in classes 1,2,3 and all 4 classes, respectively.

The link status in each class involves 3 types of events: idle channel, successful transmissions, and failed transmissions. The interactions among  $C$  classes involve  $3^C$  combinations of terms in order to calculate the average time per successful transmission. When  $C = 4$ , this is equal to  $3^4 = 81$

terms which are too complex to present analytically. Next, we design an efficient method to evaluate such combinations for  $C = 2, 3, 4$ , respectively.

Define  $T_{act,C}(S)$  as the average channel busy duration when a class  $c$  link (for  $c = 1, 2, 3, 4$ ) is active at cell  $S$ . We derive it as

$$T_{act,C}(S) = \frac{P_{suc,C}(S)T_{suc,C} + P_{F,C}(S)T_{F,C}}{1 - P_{I,C}(S)}, \quad (17)$$

where  $P_{suc,C}(S) = n_c \tau_{c,S} (1 - \tau_{c,S})^{(n_c-1)}$  and  $P_{F,C}(S) = 1 - P_{I,C}(S) - P_{suc,C}(S)$  are the successful and failed transmission probabilities of class  $c$  at cell  $S$ , respectively. Below, we suppress the index  $S$  of  $T_{act,C}$  and  $P_{I,C}$  when there is no confusion. We get:

$$\begin{aligned} T_{TX,12} &= P_{I,1}(1 - P_{I,2})T_{act,2} + P_{I,2}(1 - P_{I,1})T_{act,1} \\ &\quad + (1 - P_{I,2})(1 - P_{I,1}) \max\{T_{F,1}, T_{F,2}\}, \end{aligned} \quad (18)$$

where the first term on the right hand side (RHS) is for an active transmission event of class 2 (when the class 1 system is idle), the second term is for active event of only class 1, and the third term is for the case that both classes 1 and 2 are active. Furthermore, we obtain

$$\begin{aligned} T_{TX,123} &= \sum_{c_1=1}^3 \prod_{\substack{c_2=1 \\ c_2 \neq C_1}}^3 (1 - P_{I,C_1}) P_{I,C_2} T_{act,C_1} \\ &\quad + \sum_{c_1=1}^3 \sum_{\substack{c_2=1 \\ c_2 \neq C_1}}^3 \sum_{\substack{c_3 \neq C_1 \\ c_3 \neq C_2}}^3 (1 - P_{I,C_1})(1 - P_{I,C_2}) \\ &\quad \cdot P_{I,C_3} \max\{T_{F,C_1}, T_{F,C_2}\} \\ &\quad + (1 - P_{I,1})(1 - P_{I,2})(1 - P_{I,3}) \max\{\{T_{F,C}\}_{c=1,2,3}\}, \end{aligned}$$

where the first term on the RHS is for the active transmission event of only one class, the second term represents the case of two active classes, and the third term is for the case that all three classes are active. Finally,

$$\begin{aligned} T_{TX,1234} &= \sum_{c_1=1}^4 (1 - P_{I,C_1}) \left[ \prod_{\substack{c_2=1 \\ c_2 \neq C_1}}^4 P_{I,C_2} \right] T_{act,C_1} \\ &\quad + \sum_{c_1=1}^4 \sum_{\substack{c_2=1 \\ c_2 \neq C_1}}^4 \left[ \prod_{\substack{c_3 \neq C_1 \\ c_3 \neq C_2}}^4 P_{I,C_3} \right] (1 - P_{I,C_1}) \\ &\quad \cdot (1 - P_{I,C_2}) \max\{T_{F,C_1}, T_{F,C_2}\} \\ &\quad + \sum_{c_1=1}^4 P_{I,C_1} \left[ \prod_{\substack{c_2=1 \\ c_2 \neq C_1}}^4 (1 - P_{I,C_2}) \right] \max\{\{T_{F,C_2}\}_{c_2 \neq C_1}\} \\ &\quad + \prod_{c_1=1}^4 (1 - P_{I,C_1}) \max\{\{T_{F,C_1}\}_{c_1=1,2,3,4}\}, \end{aligned}$$

where the first to the fourth terms on the RHS are for active transmission events of any one class only, of any two

classes only, of any three classes only, and of all four classes, respectively. By using (14)–(16), the sum throughput of each class can be accurately evaluated.

## V. NUMERICAL RESULTS

In this section, we provide both analytical and simulation results for an LAA downlink system with several priority classes. We implemented computer programming on the LAA algorithms, taking into account the diverse AIFSs, CW sizes, and payload durations. The simulation results were obtained by running for  $10^6$  time slots on each parameter setting to obtain average statistics. Every analytical curve shown in this section is accompanied by a simulation curve and verified. Saturated traffic is assumed for all nodes. The spectrum sensing in the LTE-LAA system is assumed to be perfect (no hidden node problem, no false alarm or missed detection). To compare the achievable performance of different classes, time efficiency throughput is used, which is defined as the time portion of successful payload transmissions over the total simulation time. We consider two access schemes for the LAA system, a basic access scheme, and a request-to-send and clear-to-send (RTS/CTS) type of handshaking scheme. Note that downlink and uplink two-way unlicensed transmissions have been included in a recent LAA specification [3], which makes the RTS/CTS scheme more feasible to implement.

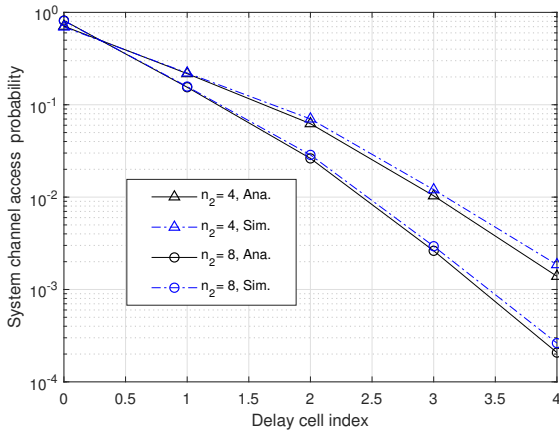


Fig. 3: System channel access probability vs. cell index of three access classes in an LTE-LAA system, when  $A_1 = A_2 = 1$ ,  $A_3 = 3$ ,  $n_1 = 2$ ,  $n_2 = 4$  or  $8$ ,  $n_3 = 10$ ,  $W_{1,0} = 4$ ,  $W_{2,0} = 8$ ,  $W_{3,0} = 16$ ,  $K_1 = K_2 = 1$ ,  $K_3 = 2$ ,  $T_{P,1} = 2$  ms,  $T_{P,2} = 3$  ms, and  $T_{P,3} = 8$  ms, with RTS/CTS.

First, we study the QoS performance of the first three classes with parameters taken from Table II. We provide the SCAP (or cell exit probability) in Fig. 3 and the time efficiency throughput in Fig. 4. The result in Fig. 3 shows that as cell index  $S$  increases, the SCAP drops sharply. This demonstrates that when the AIFS difference between classes 1 and 3 is only 2, a class 3 link only has a very small chance of transmission.

Fig. 4 shows that as  $n_2$  increases, class 2 links have increased sum throughput, but the throughput of class 3 links decrease significantly. A class 4 link based on Table II is not

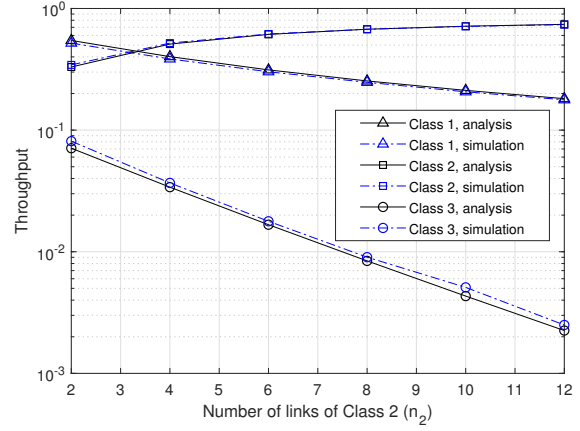


Fig. 4: Throughput of the first 3 classes in an LTE-LAA system, when  $n_2$  increases from 2 to 12, and the other parameters are the same as those used for Fig. 3.

shown here because its throughput is too low to be simulated reliably when higher priority classes have saturated traffic.

Next, to show the generality of our result, we consider a customized setup with 4 classes with different AIFS numbers  $A_1 = 1$ ,  $A_2 = 2$ ,  $A_3 = 3$ , and  $A_4 = 4$ . We provide the stationary cell probability  $P_S$  in Fig. 5, which shows that as  $S$  or  $n_2$  increases, the  $P_S$  may drop significantly. This shows that the CW size and cutoff stage setup of higher priority classes, in addition to the AIFS numbers, is critical to the achievable performance of lower priority classes.

Fig. 6 provides the sum throughput of the 4 classes. In computing the analytical throughput in Figs. 4 and 6, we used formulas from (14) and (15), respectively. As  $n_2$  increases from 2 to 12, the sum throughput of class 3 and 4 links decreases significantly. Yet, class 4 links have a much lower sum throughput than other classes, about two orders of magnitude lower than that of class 3. Note that in the majority of available analytical results on distinct AIFSs, the throughput results of lower classes (with a higher AIFS number) were plotted in a linear scale, which causes the low-value detail to be ignored. Based on our new method, we can reliably evaluate the differentiated QoS performance for low-priority classes in practical parameter range. Thus, we show our results in the logarithm scale to highlight the impact of the AIFS on the throughput in even a very low value range (e.g.  $10^{-5}$ ).

## VI. CONCLUSION

The use of diverse AIFSs to provide differentiated QoS have been included in the IEEE 802.11 WLAN, 3GPP LTE-LAA, and ETSI unlicensed spectrum access standards. The AIFS setup significantly impacts the channel access priority. In this paper, following a recent 3GPP LAA channel access specification, we have provided accurate modelling and performance analysis of the LTE-LAA priority classes. We have developed a flexible analytical approach to evaluate the transmission probability, collision probability, and time-efficiency throughput. We have implemented programming of LAA algorithms and

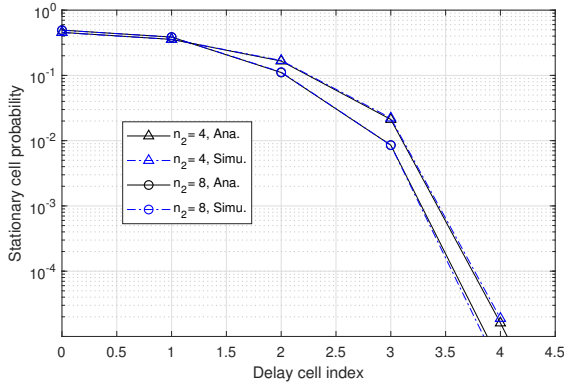


Fig. 5: Stationary cell probability vs. cell index of four access classes in an LTE-LAA system, when  $A_1 = 1$ ,  $A_2 = 2$ ,  $A_3 = 3$ ,  $A_4 = 4$ ,  $n_1 = 2$ ,  $n_3 = 10$ ,  $n_4 = 40$ ,  $W_{1,0} = W_{2,0} = W_{3,0} = W_{4,0} = 16$ ,  $K_1 = K_2 = K_3 = K_4 = 0$ ,  $T_{P,1} = 3$  ms, and  $T_{P,2} = T_{P,3} = T_{P,4} = 8$  ms, with basic access.

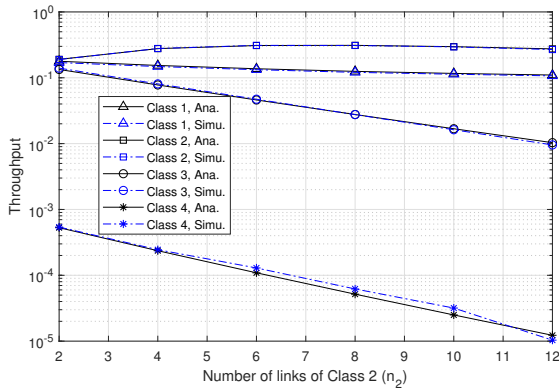


Fig. 6: Throughput of the four classes in an LTE-LAA system, when  $n_2$  increases from 2 to 12, and the other parameters are the same as those used for Fig. 5.

extensive Monte Carlo simulations, which have verified the accuracy of our analytical results, even at very low throughput as found in lower priority classes. In future work, we will study the extension of this method to other systems, such as an ETSI unlicensed spectrum access system, and coexisting LTE-LAA and WLAN systems. Furthermore, measurement and testing procedure will be implemented to further validate the analytical and simulation results.

## REFERENCES

- [1] R. Zhang, M. Wang, L. X. Cai, Z. Zheng, and X. Shen, "LTE-unlicensed: the future of spectrum aggregation for cellular networks," *IEEE Wireless Commun.*, vol. 22, no. 3, pp. 150–159, Jun. 2015.
- [2] A. Mukherjee et al., "Licensed-assisted access LTE: coexistence with IEEE 802.11 and the evolution toward 5G," *IEEE Commun. Mag.*, vol. 54, no. 6, pp. 50–57, Jun. 2016.
- [3] 3GPP TS RAN, "E-UTRA Physical Layer Procedures (Release 14)," 3GPP TS 36.213 V14.4.0, Sept. 2017.
- [4] 3GPP TSG RAN, "Study on Licensed-Assisted Access to Unlicensed Spectrum", 3GPP TR 36.889 V13.0.0, Jun. 2015.

- [5] IEEE WG802.11 Wireless LAN Working Group, "IEEE Std. 802.11e-2005 Part 11: Wireless LAN Medium Access Control (MAC) and Physical Layer (PHY) Specifications: Amendment 8: Medium Access Control (MAC) Quality of Service Enhancements," Sep. 2005.
- [6] IEEE LAN/MAN Standards Committee, "IEEE Std 802.11-2012, Part 11: Wireless LAN Medium Access Control (MAC) and Physical Layer (PHY) Specifications," Feb. 2012.
- [7] ETSI EN 301 893 V2.1.1 (2017-05), "5 GHz RLAN; Harmonised Standard Covering the Essential Requirements of Article 3.2 of Directive 2014/53/EU," May 2017.
- [8] C. Chen, R. Ratasuk, and A. Ghosh, "Downlink performance analysis of LTE and WiFi coexistence in unlicensed bands with a simple listen-before-talk scheme," in *Proc. IEEE VTC*, Glasgow, May 2015, pp. 1–5.
- [9] Y. Song, K. W. Sung, and Y. Han, "Coexistence of Wi-Fi and cellular with listen-before-talk in unlicensed spectrum," *IEEE Commun. Lett.*, vol. 20, no. 1, pp. 161–164, Jan. 2016.
- [10] A. K. Ajami and H. Artail, "Fairness in future licensed assisted access (LAA) LTE networks: What happens when operators have different channel access priorities?" in *Proc. IEEE ICC Workshops*, Paris, May 2017, pp. 67–72.
- [11] Y. Ma and D. G. Kuester, "MAC-Layer Coexistence Analysis of LTE and WLAN Systems Via Listen-Before-Talk," in *Proc. IEEE CCNC*, Las Vegas, Jan. 2017, pp. 534–541.
- [12] Y. Ma, D. G. Kuester, J. Coder, and W. F. Young, "Coexistence analysis of LTE and WLAN systems with heterogenous backoff slot durations", in *Proc. IEEE ICC*, Paris, May 2017, pp. 1–7.
- [13] Y. Ma, R. Jacobs, D. G. Kuester, J. Coder, and W. F. Young, "SDR-Based experiments for LTE-LAA based coexistence systems with improved design," in *Proc. IEEE GlobeCom*, Singapore, Dec. 2017, pp. 1–6.
- [14] V. Valls, A. Garcia-Saavedra, X. Costa and D. J. Leith, "Maximizing LTE capacity in unlicensed bands (LTE-U/LAA) while fairly coexisting with 802.11 WLANs," in *IEEE Commun. Lett.*, vol. 20, no. 6, pp. 1219–1222, Jun. 2016.
- [15] R. Yin, G. Yu, A. Maaref, and G. Li, "A framework for co-channel interference and collision probability tradeoff in LTE licensed-assisted access networks," *IEEE Trans. Wireless Commun.*, vol. 15, no. 9, pp. 6078–6090, Sept. 2016.
- [16] S. Han, Y. C. Liang, Q. Chen and B. H. Soong, "Licensed-assisted access for LTE in unlicensed spectrum: A MAC protocol design," in *Proc. IEEE ICC*, Kuala Lumpur, Malaysia, May 2016, pp. 1–6.
- [17] S. Han, Y. C. Liang, Q. Chen and B. H. Soong, "Licensed-assisted access for LTE in unlicensed spectrum: A MAC protocol design," *IEEE J. Sel. Areas Commun.*, vol. 34, no. 10, pp. 2550–2561, Oct. 2016.
- [18] Jie Hui and M. Devetsikiotis, "A unified model for the performance analysis of IEEE 802.11e EDCA," *IEEE Trans. Commun.*, vol. 53, no. 9, pp. 1498–1510, Sept. 2005.
- [19] J. Y. Lee and H. S. Lee, "A performance analysis model for IEEE 802.11e EDCA under saturation condition," *IEEE Trans. Commun.*, vol. 57, no. 1, pp. 56–63, Jan. 2009.
- [20] J. Y. Lee, H. S. Lee and J. S. Ma, "Model-based QoS parameter control for IEEE 802.11e EDCA," *IEEE Trans. Commun.*, vol. 57, no. 7, pp. 1914–1918, July 2009.
- [21] I. Tinnirello and G. Bianchi, "Rethinking the IEEE 802.11e EDCA performance modeling methodology," *IEEE/ACM Trans. Netw.*, vol. 18, no. 2, pp. 540–553, April 2010.
- [22] Y. Gao, X. Sun and L. Dai, "IEEE 802.11e Std EDCA networks: modeling, differentiation and optimization," *IEEE Trans. Wireless Commun.*, vol. 13, no. 7, pp. 3863–3879, July 2014.
- [23] L. Dai and X. Sun, "A unified analysis of IEEE 802.11 DCF networks: stability, throughput, and delay," *IEEE Trans. Mobile Computing*, vol.12, no.8, pp.1558–1572, Aug. 2013.
- [24] G. Bianchi, "Performance analysis of the IEEE 802.11 distributed coordination function," *IEEE J. Sel. Areas Commun.*, vol. 18, no. 3, pp. 535–547, Mar. 2000.